Electronic Supplementary Information for Dalton Transactions

Supplementary Information (ESI)

Comparative study of the catalytic activity of $[Mn^{II}(bpy)_2Cl_2]$ and $[Mn_2^{III/IV}(\mu\text{-}O)_2(bpy)_4](ClO_4)_3$ in the H_2O_2 induced oxidation of organic dyes in carbonate buffered aqueous solution

Sabine Rothbart, Erika Ember and Rudi van Eldik*

Reaction of the $[Mn(bpy)_2Cl_2]$ and $[Mn_2(\mu\text{-}O)_2(bpy)_4](ClO_4)_3$ catalyzed oxidation of Morin and *p*-nitrophenol by H_2O_2 in carbonate buffered solution at pH 9.0

In agreement with the results obtained for Orange II, the oxidation course with Morin and *p*-nitrophenol as substrate show identical reactivity for the *in situ* formed catalyst as well as for the readily prepared catalysts $[Mn^{II}(bpy)_2Cl_2]$ and $[Mn_2(\mu\text{-}O)_2(bpy)_4](ClO_4)_3{\cdot}2H_2O$. In the case of flavonoidic compounds such as Morin, it is known that upon oxidation an initial increase followed by the oxidative decay at 330 nm can be observed, whereas at 400 nm the decay of the phenolic part starts immediately. This is due to the extension of the π-system of the dye, which results in an initial intensification of the corresponding absorbance, as it is often observed for flavonoidic dyes.

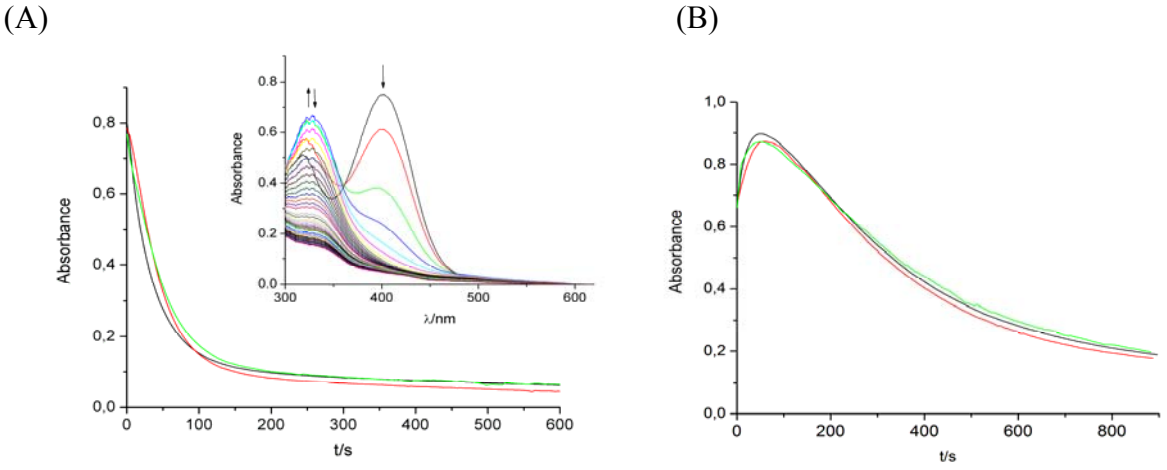

Fig. S1. Observed spectral changes (inset A) and kinetic traces recorded at 400 nm (A) and 330 nm (B) for the degradation of Morin. Reaction conditions: 0.1 M HCO_3^-, 5 x 10^{-5} M Morin, 0.015 M H_2O_2, pH 9.0, room temp., (—) 4 x 10^{-5} M $[Mn^{II}(bpy)_2Cl_2]$, (—) 2 x 10^{-5} M $[Mn_2^{III/IV}(\mu\text{-}O)_2(bpy)_4](ClO_4)_3$, (—) 4 x 10^{-5} M $MnCl_2$ + 8 x 10^{-5} M bpy.

Under the selected reaction conditions, only partial oxidation of *p*-nitrophenol is possible (400 nm), since the parallel decomposition of H_2O_2 results in a sudden disruption of the reaction course. Addition of a second portion of H_2O_2 would restart the oxidation process again (see Figure S8 (B)). This can be avoided when lower catalyst concentrations are used, although this leads to a drastic decrease in reactivity, as can be seen from the corresponding kinetic traces.

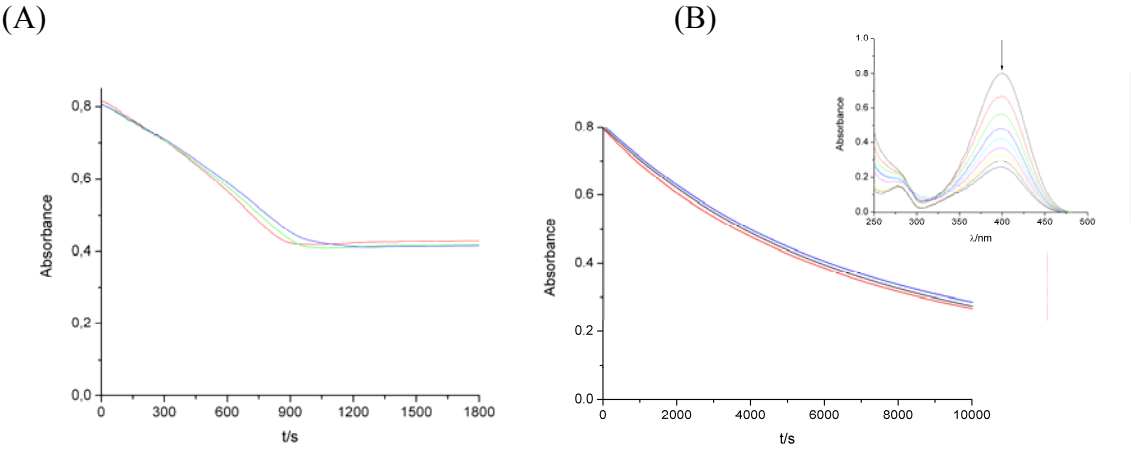

Fig. S2. Kinetic traces recorded at 400 nm for the degradation of *p*-nitrophenol. Reaction conditions: 0.1 M HCO_3^-, 5 x 10^{-5} M *p*-nitrophenol, pH 9.0, room temp., (A): 0.015 M H_2O_2, (—) 4 x 10^{-5} M $[Mn^{II}(bpy)_2Cl_2]$, (—) 2 x 10^{-5} M $[Mn_2^{III/IV}(\mu\text{-}O)_2(bpy)_4](ClO_4)_3$, (—) 4 x 10^{-5} M $MnCl_2$ + 8 x 10^{-5} M bpy; (B): 0.01M H_2O_2, (—) 5 x 10^{-6} M $[Mn^{II}(bpy)_2Cl_2]$, (—) 2.5 x 10^{-6} M $[Mn_2^{III/IV}(\mu\text{-}O)_2(bpy)_4](ClO_4)_3$, (—) 5 x 10^{-6} M $MnCl_2$ + 1 x 10^{-5} M bpy and corresponding spectral changes (inset B).

Verification of pH profile for the oxidation of *p*-nitrophenol

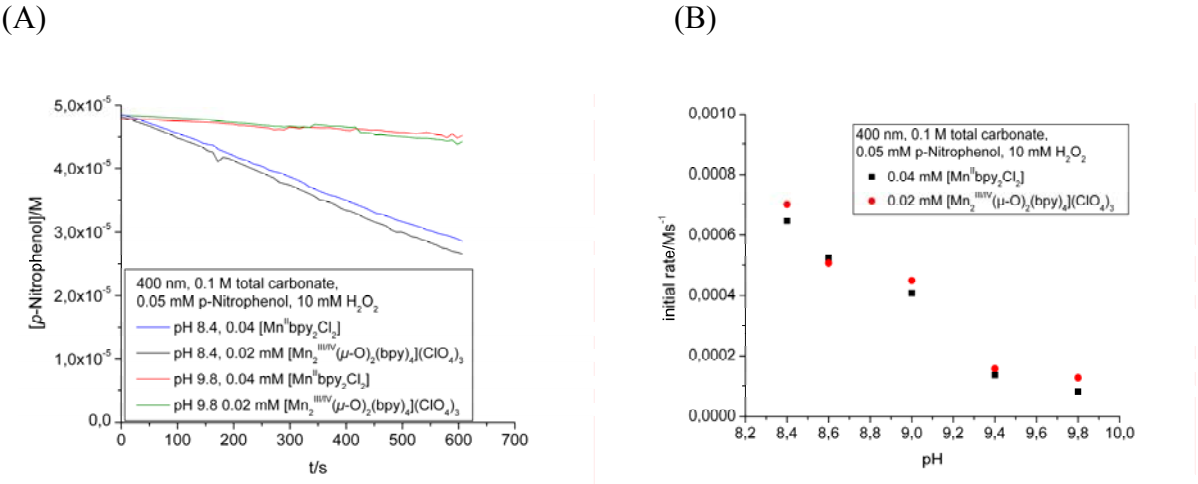

Fig. S3. (A) Kinetic traces recorded at 400 nm for the degradation of *p*-nitrophenol at different pH values. (B) pH dependence of the initial rate of *p*-nitrophenol bleaching (■) 4 x 10^{-5} M $[Mn^{II}(bpy)_2Cl_2]$, (●) 2 x 10^{-5} M $[Mn_2^{III/IV}(\mu\text{-}O)_2(bpy)_4](ClO_4)_3$. Reaction conditions: 0.1 M HCO_3^-, 5 x 10^{-5} M *p*-nitrophenol, 0.01 M H_2O_2, room temp..

Control experiments at different ionic strengths and influence of the counter ion

Control experiments at different ionic strengths (adjusted with $NaNO_3$) and additional NaCl at constant bicarbonate concentrations showed no influence of ionic strength or the counter ion on the observed reaction course.

(A) (B)

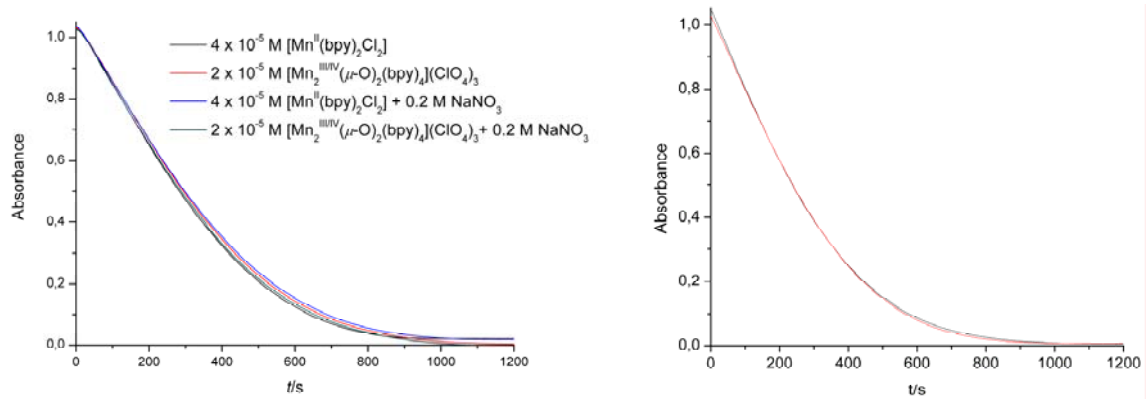

Fig. S4. Kinetic traces recorded for the oxidation of 5 x 10^{-5} M Orange II by (A) 4 x 10^{-5} M $[Mn^{II}(bpy)_2Cl_2]$ and 2 x 10^{-5} M $[Mn_2^{III/IV}(\mu\text{-}O)_2(bpy)_4](ClO_4)_3$ in the presence of 0.1 M HCO_3^- and 0.015 M H_2O_2, compared to the same reaction in the presence of 0.2 M $NaNO_3$; (B) 4 x 10^{-5} M $[Mn^{II}(bpy)_2Cl_2]$ in the presence of 0.1 M NaCl. Reactions followed at 484 nm, pH 9.0, room temp., over 20 min.

Oxidation reaction in the absence of carbonate

In response to critical comments, we performed the oxidation reaction in the absence of carbonate buffer in order to assure the involvement of *in situ* formed peroxycarbonate. The oxidation reaction was therefore performed under identical reaction conditions without any carbonate present in solution, but in CHES buffered solution at pH 9.0. In Figure S5 the catalyzed oxidation reaction of Orange II for either of the catalysts in the absence of carbonate (c), is compared with the same experiments in 0.1 M (b) and 0.3 M (a) carbonate buffered solution under identical reaction conditions. Although the reaction of the manganese catalysts with HOO^- (note that the pK_a value of H_2O_2 is 11.3) could in general be possible, the tremendous rate enhancement by carbonate on the catalyzed oxidation reaction of Orange II becomes evident for both of the catalysts. Thus the formation of peroxycarbonate is essential to account for the observed reaction rate and the dependence on the carbonate concentration.

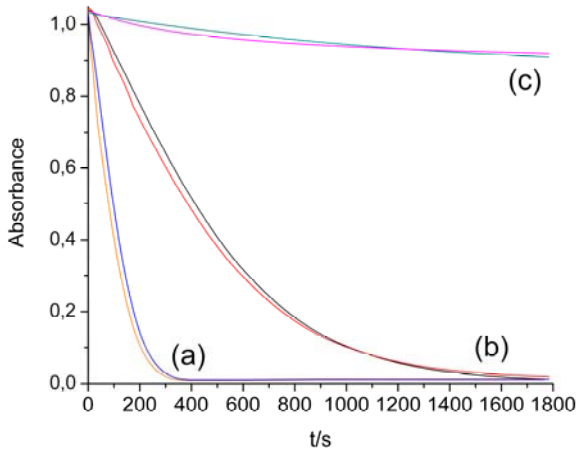

Fig. S5. Kinetic traces recorded for the oxidation of 5 x 10^{-5} M Orange II by 4 x 10^{-5} M $[Mn^{II}(bpy)_2Cl_2]$ and 2 x 10^{-5} M $[Mn_2^{III/IV}(\mu\text{-}O)_2(bpy)_4](ClO_4)_3$ in the presence of 0.01 M H_2O_2 and (A) 0.1 M HCO_3^- at pH 9.0 (B) 0.3 M HCO_3^- at pH 9.0, compared to the same reaction in the absence of any carbonate in 0.1 M CHES buffer (C). Reactions conditions: pH 9.0, room temperature.

Catalyst dependence of the reaction course for $[Mn^{II}(bpy)_2Cl_2]$ and $[Mn_2(\mu\text{-}O)_2(bpy)_4](ClO_4)_3$

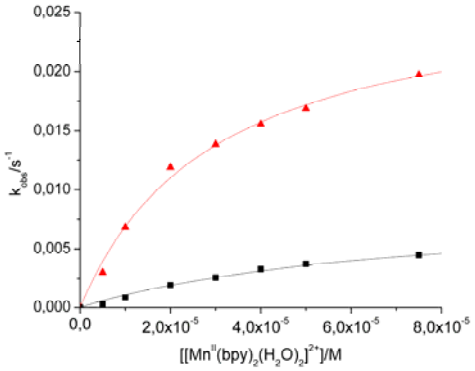

Fig. S6. Observed rate constants measured at 484 nm as a function of $[Mn^{II}(bpy)_2(H_2O)_2]^{2+}$ concentration at different total carbonate concentrations. Reaction conditions: 0.01 M H_2O_2, 5 x 10^{-5} M Orange II, pH 9.0, room temp., (■) 0.1 M HCO_3^-, (▲) 0.5 M HCO_3^- .

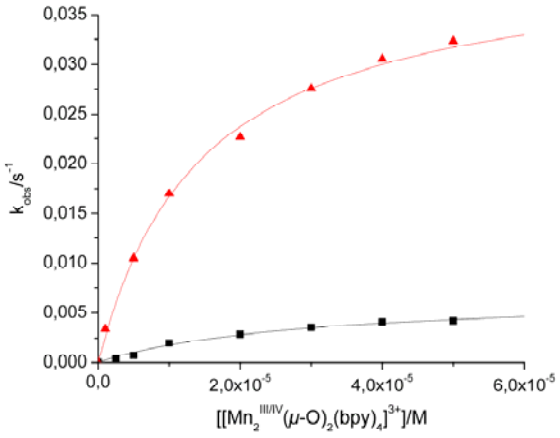

Fig. S7. Observed rate constants measured at 484 nm as a function of $[Mn_2^{III/IV}(\mu\text{-}O)_2(bpy)_4]^{3+}$ concentration at different total carbonate concentrations. Reaction conditions: 0.01 M H_2O_2, 5 x 10^{-5} M Orange II, pH 9.0, room temp., (■) 0.1 M HCO_3^-, (▲) 0.5 M HCO_3^-.

Control EPR experiments in the presence of ^{t}BuOH at different $[H_2O_2]$

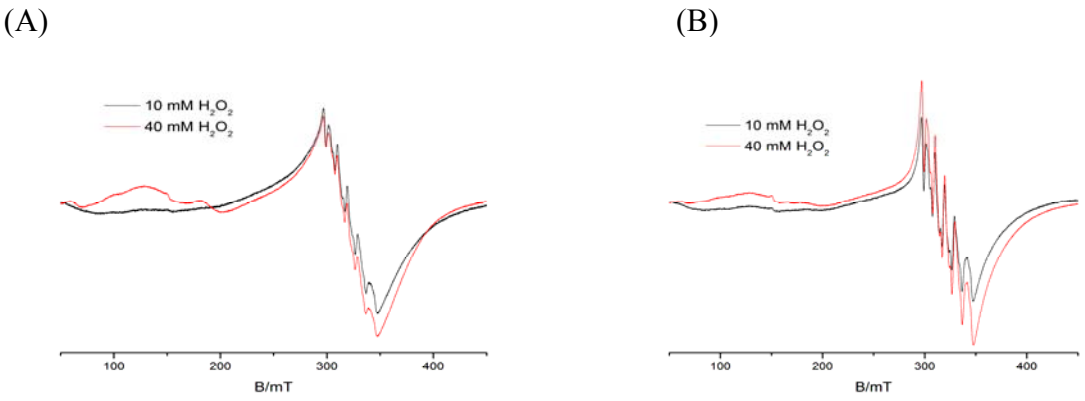

Fig. S8. X-band EPR spectra of 0.1 M bicarbonate containing solutions of H_2O:^{t}BuOH (1:1). Reaction conditions: pH 9.0, room temp., (A) 1 x 10^{-4} M $[Mn^{II}bpy_2Cl_2]$ and (B) 5 x 10^{-5} $[Mn_2O_2(bpy)_4](ClO_4)_3$ with (—) 0.01 M and (—) 0.04 M H_2O_2 immediately after mixing. EPR conditions: 8.98 GHz, 6 K, 1 mW microwave power, modulation amplitude 20 mT.

UV/Vis spectra of the reaction of $[Mn_2(\mu\text{-}O)_2(bpy)_4](ClO_4)_3$ with H_2O_2 in carbonate buffered solution

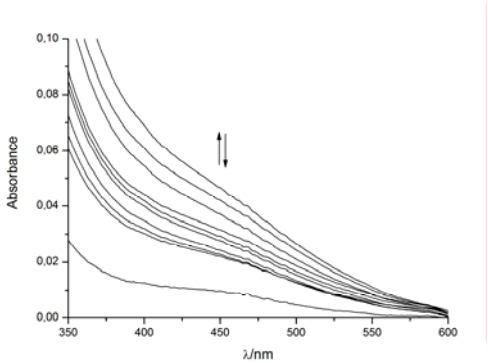

Fig. S9. Spectral changes recorded for the reaction of 0.05 x 10^{-3} M $[Mn_2(\mu\text{-}O)_2(bpy)_4](ClO_4)_3$ with 5 x 10^{-3} M H_2O_2 in 0.1 M HCO_3^- solution; spectra recorded in time intervals of 0.2 s for the first two seconds, pH 9.0, room temp.

Dependence of the reaction course on the ligand-to-Mn ratio for Morin and *p*-nitrophenol

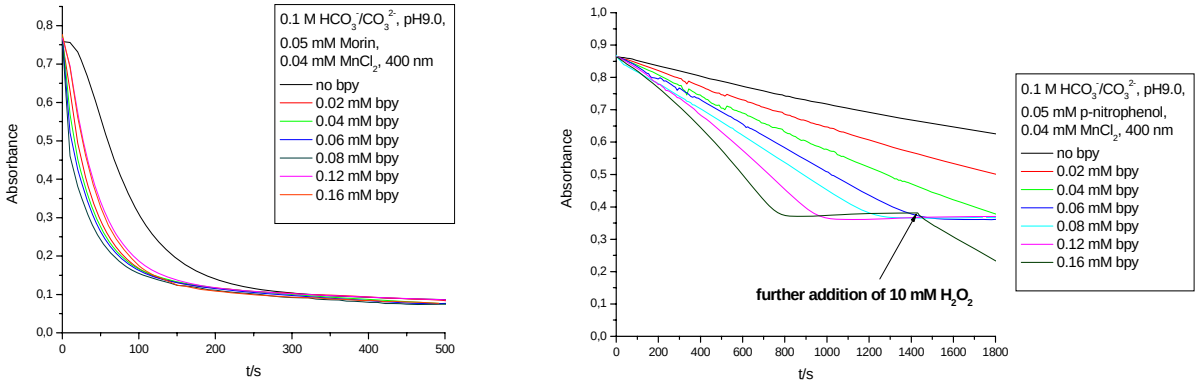

Fig. S10. Kinetic traces recorded at 400 nm for the *in situ* oxidation of Morin (A) and *p*-nitrophenol with 4 x 10^{-5} M $MnCl_2$ and increasing amount of 2,2'-bipyridine added to the reaction mixture. Reaction conditions: 0.1 M bicarbonate, between 0.5-4 % CH_3CN, 5 x 10^{-5} M dye, 0.015 M H_2O_2, pH 9.0, room temperature.